Journal of Magnetic Resonance **144,** 217–227 (2000)
doi:10.1006/jmre.2000.2075, available online at http://www.idealibrary.com on IDEAL®

Changes in ADC Caused by Tensile Loading of Rabbit Achilles Tendon: Evidence for Water Transport

S. Han,* S. J. Gemmell,* K. G. Helmer,* P. Grigg,† J. W. Wellen,* A. H. Hoffman,‡ and C. H. Sotak*,§,¶

**Department of Biomedical Engineering, §Department of Chemistry and Biochemistry, and ‡Department of Mechanical Engineering, Worcester Polytechnic Institute (WPI), Worcester, Massachusetts 01609; and †Department of Physiology and ¶Department of Radiology, University of Massachusetts Medical School and UMassMemorial Healthcare, Worcester, Massachusetts 01655*

Received August 26, 1999; revised February 10, 2000

Water diffusion measurements were performed on rabbit Achilles tendons during static tensile loading and tendons in an unloaded state. The apparent diffusion coefficient (ADC) was measured along two directions: parallel and perpendicular to the long axis of the tendon. Tendons were studied after being prepared in two ways: (a) after being stored frozen in phosphate-buffered saline (PBS) and (b) freshly isolated. Statistically significant directional anisotropy was observed in the ADC in all tendons. The ADC was significantly greater in the direction parallel to the long axis of the tendon than in the perpendicular direction. The anisotropy is attributed to the greater restrictions seen by the water molecules in the perpendicular direction and is consistent with the known geometry of the tendon. Storage in PBS caused tendons to swell. This increased the ADC measured along both directions and reduced the anisotropy. The existence of anisotropy in the ADC was not related to the orientation of the specimen in the magnet. The ADC increased along both directions following the application of a 5-N tensile load; the increase was greatest along the perpendicular axis of the tendon. In order to determine whether load-related changes in the ADC reflected changes in interfibrilar spacing, we used electron microscopy to measure load-related changes in fibril spacing. Load-related changes in fiber spacing could not account for the observed changes in the ADC. The increase in ADC caused by loading was attributed to the extrusion of tendon water into a bulk phase along the outside surface of the tendon. In PBS-stored samples, enough fluid was extruded that it could be visualized. The transient response of the ADC to a 5-N tensile load was also studied. The absolute ADC in both directions increased with loading and recovered to baseline upon unloading. The transient changes in ADC, for both loading and unloading, had a mean time constant of approximately 15 min. The magnitude of the load-induced transient ADC changes was comparable to that seen in the static-loading experiments.

Key Words: **tendon; water transport; anisotropy; ADC; tensile loading.**

INTRODUCTION

There is considerable evidence that the water contained in biological soft tissue structures plays an important role in determining the way those materials respond when they are mechanically loaded. For example, when cartilage is compressed, there is movement of water through the solid matrix of the cartilage (*1*). The fluid resistance associated with this water movement through tortuous paths in the solid matrix creates a viscous component in the load response. In addition, the static material properties of soft tissues loaded in tension are strongly influenced by changes in tissue hydration (*2–5*). It is also known that the viscoelastic properties of tissues are changed by hydration (*6*).

While an important role for water is suggested by the above studies, there have been experimental obstacles to studying water content or water movement in tissues. For example the water content of a sample can be measured by weighing it while wet and again after drying it in an oven (*7*). However, a fundamental problem with this method is that it is destructive; only one observation can be obtained from each sample.

In this report we describe a nondestructive method, based on NMR measures of the apparent diffusion coefficient (ADC) of water, to demonstrate fluid movement caused by tensile loading of rabbit Achilles tendons.

The ADC can be measured using pulsed-field-gradient (PFG) NMR. Since the mean-squared displacement of water molecules is reduced by the presence of physical barriers, the ADC magnitude, at a given diffusion time, reflects the proximity of barriers encountered by water molecules as they diffuse. Tendons are made up of long, parallel arrays of collagen molecules, which assemble to make parallel arrays of collagen fibrils, which in turn assemble to make gross tendons. Since these components constitute barriers to diffusion, changes in their spacing are reflected in the ADC measurement.

Diffusion in the presence of barriers or "restricted diffusion" is determined by the relative magnitudes of the diffusion length, l_d, and the size of the space available for diffusion, the structure length, l_s (*8*). The diffusion length is the average distance that molecules can diffuse in a given diffusion time, $l_d = (\mathrm{ADC} \times t)^{1/2}$, where t is the diffusion time. When $l_d \ll l_s$, a majority of molecules will not have diffused far enough to experience restrictions imposed by the barriers. However, as t

1090-7807/00 $35.00

is increased, an increasing number of molecules will have their motion restricted and the measured ADC will be reduced from D_0, the diffusion coefficient of the bulk fluid. In this regime, the ADC can reflect average measures of the barrier spacing, such as the ratio of the medium's surface-area to volume (*9*). For the case of $l_d \gg l_s$, molecules have fully experienced the restricted diffusion space and now the measured ADC reflects the connectivity of the diffusion species in the medium (*10*). The barrier spacings to which PFG NMR experiments are sensitive are therefore determined by l_d. For example, if the barrier spacing is L, the diffusion time must be such that a majority of water molecules have diffused that far during the measurement in order that the effect of the barriers is fully reflected in the measured ADC. The diffusion times used in these experiments ranged from 6.5 to 148.5 ms. The largest ADC measured in these experiments was 14×10^{-6} cm^2/s, so barrier spacings less than 1 μm were not detectable. The majority of the diffusing water molecules would have experienced the restrictions due to such barriers during the minimum 6.5-ms diffusion time. While the ADC is sensitive to packing at the $>$1-μm level, it may nonetheless be influenced by changes in the packing beyond its resolution limit, e.g., at the fibrillar level. For example, increasing the closeness of packing at the fibrillar level could cause water to be displaced to another location, such as a bulk phase, outside the tendon, where it experiences different barriers to diffusion. If such a bulk phase is contained within the volume sampled during an ADC measurement, then it will influence the resulting value of ADC. If it can be shown that packing does not change significantly (i.e., by an order of magnitude) at the micrometer level, then changes in the ADC can be used to make inferences about water transport associated with tensile loading.

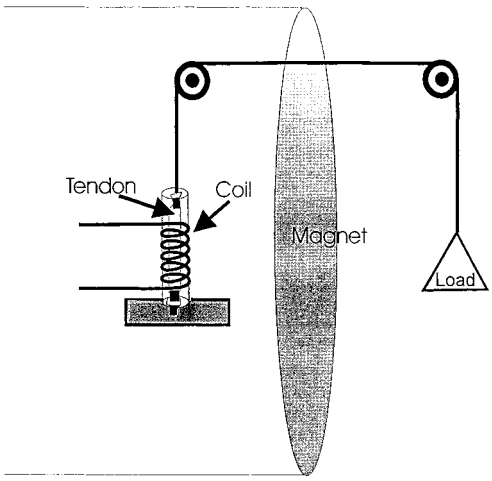

FIG. 1. Experimental apparatus for the ADC measurements. The tendon is held in a paraffin-oil-filled plastic tube, mounted in the bore of the magnet perpendicular to the main magnetic field, and attached to the applied load with suture material that is led outside the magnet over pulleys. The load is applied outside the magnet. The solenoid RF coil is placed around the outside of the plastic tube.

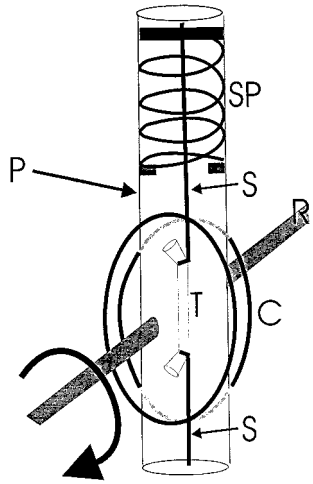

FIG. 2. Apparatus for measuring the effect of tendon orientation on the ADC. The tendon (T) is held in a Lucite tube (P) with suture material (S). The tendon is held under tension by the spring (SP). The tube can be rotated about the shaft (R) to change the orientation in the magnet. A Helmholtz RF coil (C) pair was used with this apparatus.

METHODS

1. Tendon Preparation

Studies were conducted using Achilles tendons from young (3 kg) New Zealand white rabbits of either sex. Just prior to initiating the experiment, rabbits were euthanized with an overdose of Nembutal, and Achilles tendons were dissected from the hindlimbs. The dissection was done in a closed chamber that was maintained at 100% humidity, in order to prevent dehydration of the tendons. The gross Achilles tendons were removed from each leg; each was divided longitudinally into three individual tendons. Each individual tendon was tied at its ends with No. 0 surgical thread that was used to mount the tendon in the apparatus. The tendons were then stored in paraffin oil until used. All tendons were studied within 3.5 h of harvesting.

In a set of initial experiments, tendons were dissected in an open environment and stored frozen in 300 mOsm phosphate-buffered saline (PBS) solution at pH 7.4. They were thawed just prior to use in the experiment. There were some differences (noted below) in experimental procedures in the experiments using fresh and PBS-stored tendons.

2. Apparatus

ADC measurements were made using the apparatus shown in Fig. 1. Tendons were mounted vertically, normal to the magnet bore in a section of Lucite tubing with 5.3-mm inside diameter. The tubing was filled with paraffin oil to prevent tendon dehydration. The RF coil was a nine-turn solenoid that conformed to the outside of the tubing. When mounted in the apparatus, the tendon extended approximately 6 mm beyond

TABLE 1
Summary of the Pulse Sequences Used in Different Experimental Paradigms

Experimental paradigm	Measurement	Sequence(s)	
Static loading—PBS-stored tendon	Load/no load	PG SE	
Static loading—Fresh tendon	Diffusion-time dependence of ADC; load/no load	Short t	Long t
		PG SE	PG STE
Transient loading—Fresh tendon	ADC	PG STE	
Change of orientation			

Note. The parameters used in each pulse sequence are listed in Table 2.

the top and bottom ends of the RF coil. One end of the tendon was tied to the bottom of the apparatus. The string on the top end of the tendon was led, over a pulley system, to the outside of the magnet. The tendon was loaded in tension by hanging masses on the string, exterior to the magnet. Masses of approximately 0.04, 0.5, and 1.0 kg were used, resulting in tensile loads of 0.4, 5, and 10 N, respectively.

In experiments designed to test for the dependence of the ADC on the orientation of the sample in the magnet, a second apparatus was used (Fig. 2). In this apparatus, the tendon was mounted in a closed plastic tube filled with paraffin oil. The tendon was held by surgical thread that was anchored at one end and held under tension (0.4 N) by a spring arrangement at the other end. The orientation of the sample in the magnet could be changed by rotating the tube 90°. Thus, the long axis of the tube (and the tendon) could be either normal or parallel to the main magnetic field, B_0. The RF coil was a 15-mm-diameter Helmholtz coil that was concentric with the axis of rotation of the tube. The tube rotated in the plane of the Helmholtz coil.

3. ADC Measurements

All NMR measurements were made using a GE CSI-II 2.0 T/45 cm imaging spectrometer operating at 85.56 MHz for protons and equipped with ±20 G/cm self-shielded gradients. The ADC of tendon–water protons was measured spectroscopically using two pulse sequences: either a pulsed-field-gradient spin-echo (PFG SE) or a stimulated-echo (PFG STE) sequence (Tables 1 and 2). Each pulse sequence included 1:3:3:1 chemical-shift selective pulses for paraffin-oil-signal suppression (*11*). The frequency separation between the water and paraffin resonances was 312.5 Hz. The orientation, load, loading-time, and diffusion-time dependence of the ADC were determined for measurements made both parallel and perpendicular to the long axis of the tendons.

a. Effect of static tensile loading and diffusion time. The effect of tensile loading on the ADC was measured using separate methods in the preliminary and the final experiments. In the initial experiments, load-related effects on ADC were studied using tendons stored in PBS ($N = 30$). In these experiments, the ADC was first measured with the tensile load set at 0.4 N, a load sufficient to prevent slack in the tendon. The tensile load was then changed to 5 N, followed by 10 N, and then returned to 0.4 N. Each time the load was changed, no data were collected for at least 10 min, in order to allow the tissue to reach a steady state. In the final static-loading experiments, freshly isolated tendons were used ($N = 10$), and two levels of static loading (0.4 and 5 N) were used. In the final experiments, the effects of static loading and diffusion times were studied together, in order to determine any potential interaction between those two variables. Fresh tendons were placed in the magnet using the apparatus shown in Fig. 1. Pulse sequences and NMR parameters used in the above experiments are described in Tables 1 and 2.

Inversion-recovery and Hahn spin-echo methods were used to measure the T_1 and T_2 of several samples in order to determine the repetition and echo times. Typical values for the relaxation times were $T_1 = 475$ ms and $T_2 = 35$ ms.

TABLE 2
Summary of NMR Parameters Used in the Pulse Sequences Shown in Table 1

	Experiment	Gradient strength (G/cm)	TE (ms)	TR (ms)	δ (ms)	No. of avgs	t (ms)	Tensile loads
1	PBS-stored tendon—Static load	1–15	120	1000	6	2	80	0.4, 5, 10
2	Fresh tendon—Static load	3–15	25	1000	6	2	10–20	0.4, 5
3	Fresh tendon—Static load	3–15	25	1000	6	4	50–150	0.4, 5
4	Fresh tendon—Transient load	3–18	25	1750	6	4	80	0.4, 5
	Change of orientation					100		0.4

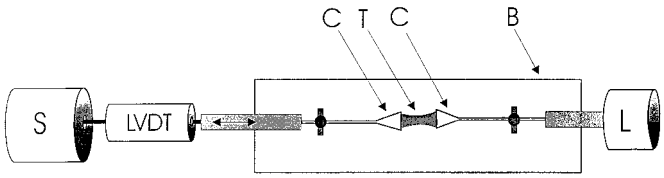

FIG. 3. Apparatus for uniaxial material testing of tendons. The tendon (T) is maintained in a paraffin oil bath (B). It is held by two clamps (C). One clamp is connected to the linear actuator (S) through a linear variable differential transformer (LVDT). The second clamp is coupled to a load cell (L).

b. Effect of transient loading. The transient response of the ADC was measured by recording it before, during the application of, and while recovering from the application of a 5-N tensile load. Upon securing the tendon to the apparatus, five measures of ADC were made with a 0.4-N load. The load was then switched to 5 N for 30 min. The ADC was measured each minute for 5 min and then at 5-min intervals thereafter. After 30 min, the load was switched back to 0.4 N for 30 min. The ADC was measured perpendicular and parallel to the tendon long axis with a PFG STE pulse sequence (Tables 1 and 2).

c. Effect of tissue orientation. Fresh tendons were mounted in the apparatus shown in Fig. 2. With the sample perpendicular to B_0, the ADC was measured in directions both perpendicular and parallel to B_0. The specimen was then rotated 90° (to position the long axis of the tendon parallel to B_0), and the same sequence was repeated. All ADC measures were made using the same pulse sequence as in the transient tests (above).

4. Mechanical Testing

In separate experiments, not utilizing NMR, tendons were studied in a tensile loading apparatus (Fig. 3) in which the mechanical responses to loading could be determined under conditions similar to those used in the NMR experiments. This apparatus has been described in detail elsewhere (*12*). Two mechanical testing paradigms were used:

a. In order to determine whether the loads we used caused physiologically relevant stresses, we characterized the stress–strain relationship for tendons using loads identical to those employed in the NMR experiments. Tendons were secured to clamps (C) coupled to a linear actuator and a load cell (L). In this device, the tendon was held horizontally; the bathing material for the tendon was paraffin oil. The temperature of the oil bath (B) was kept at 18°C, the same as the temperature measured inside the magnet. A microscope was mounted above the tendon so that its diameter and thus its cross-sectional area could be measured optically. Stresses were calculated from the applied loads and the cross-sectional area. Strains were determined by measuring the displacements of small markers fixed on the tendon surface.

b. We performed creep tests in order to determine the transient mechanical behavior of the tendons under conditions similar to those used in the NMR experiments. The magnitudes of applied loads and the duration of their application were identical to the values used in the NMR experiments. Fresh tendons were stretched using the linear actuator; force was the controlled variable. Thus, just as in the experiments in the magnet, the force was fixed while displacement varied during the trial. Displacements were recorded during a 30-min period, during which a 5-N load was applied, and during a subsequent 30-min recovery period, in which the applied load was 0.4 N. L_O was measured as the length of the tendon between the clamps at zero load; the increments in displacement measured during the test were converted to strains using a Lagrangian formulation (*13*).

5. Electron Microscopy

Four tendons were fixed with 2.5% glutaraldehyde under loaded or unloaded conditions. Two tendons were fixed while under 10.2-N tensile load and two were fixed while unloaded (0.4-N load). The tendons were maintained under tension in the fixative for 4 h. Tendons were then embedded in plastic and thin sections were cut transverse to the long axis of the tendon using a diamond knife. The resulting sections were visualized using a transmission electron microscope and photographed at 40,000×. The resulting photographs were scanned and analyzed using NIH Image software (ver. 1.55). In order to determine the distributions of fibril diameters, the sizes of all fibrils were measured (excluding those that were only partially visible because they intercepted the edges of the photographs). In order to measure interfibrillar space, the area of all fibrils (including those that intercepted the edges) was determined and subtracted from the total area of the photograph.

RESULTS

1. ADC Measures

a. ADC values in unloaded tendons. Table 3 summarizes the ADC values measured (at $t = 80.0$ ms) under unloaded (0.4-N tensile load) conditions from all experiments (i.e., on both fresh and PBS tendons). The ADC showed marked directional anisotropy: it was significantly greater along the long (parallel) axis of the tendon than along its short (perpendicular) axis. The mean anisotropy ratio (mean $ADC_{\parallel}$/mean $ADC_{\perp}$) was 1.5 for PBS-stored tendon and 2.8 for fresh tendon. Storage in PBS increased the ADC significantly, by 230% in the parallel direction, and by 436% in the perpendicular direction.

b. Effect of tensile loading and diffusion time on static ADC values. Static tensile loading caused an increase in the ADC in both fresh and PBS-stored tendons (Figs. 4 and 5). The increase was observed along both parallel and perpendicular directions. The relationship between the ADC and the magnitude of the applied load was tested in PBS-stored tendons (Fig.

TABLE 3

Tendon–Water ADC as Measured along Directions Parallel and Perpendicular to Tendon Long Axis, for both Fresh and PBS-Stored Tendons

	Fresh tendons		PBS tendons	
	Parallel	Perpendicular	Parallel	Perpendicular
Range	4.2–8.3	1.0–4.1	10.4–19.4	5.3–18.1
Mean	6.7	2.4	15.4	10.5
N	18	24	30	30
SEM	0.2	0.2	0.6	0.7

Note. All ADC values are $\times 10^6$ cm^2/s. The diffusion time for all of the measurements was 80 ms.

4). The ADC increased with increasing load and returned toward control with unloading; however, the ADC did not recover to initial values even after recovery times of up to 0.5 h. The significance of the effect of loading on the measured ADC was tested using a repeated-measures ANOVA and with specific pairwise comparisons between group means. The ANOVA revealed that the effect of loading was highly significant ($P < 0.0001$). Pairwise comparisons between group means were made within the perpendicular and parallel groups to determine which individual group means differed from each other. The only significant pairwise comparison was between 0.4- and 10-N perpendicular groups ($P < 0.01$).

The effect of varying diffusion time was tested using fresh tendons (Fig. 5). Initially, the ADC decreased with longer diffusion times; however, the ADC began again to increase as t was increased further. The anisotropy ratio calculated from the mean ADC at each diffusion time ranged from 2.3 (unloaded, $t = 8.5$ ms) to 2.1 (unloaded, $t = 148.5$ ms) and 1.8 (loaded, $t = 8.5$ ms) to 1.7 (loaded, $t = 148.5$ ms).

c. Transient effect of tensile loading. The transient response of the ADC to a 5-N tensile load was studied in 10 fresh tendons; the results are shown in Fig. 6. The ADC increased along both the parallel and the perpendicular directions during the period that the load was applied. The mean value of the increase was greater along the perpendicular direction (6.8×10^{-6} cm^2/s) than along the parallel direction (3.8×10^{-6} cm^2/s). The magnitude of the load-induced change was comparable to that seen in the static-loading experiments (e.g., see Fig. 5). The significance of changes in the ADC was evaluated using repeated-measures ANOVA by comparing the five values recorded prior to load application to the three values recorded between 20 and 30 min following load application, when the ADC change had reached a relatively steady state. The percentage increases along both directions were highly significant ($P < 0.001$).

The absolute ADC in both directions recovered to baseline upon unloading (Fig. 6). The changes in ADC had a mean time constant of approximately 15 min. The time constants did not differ between loading and unloading conditions. The transient response was not measured in PBS-stored tendons.

d. Effects of tendon orientation on ADC. The effect of tendon orientation in the magnet was studied in four fresh tendons, using the apparatus shown in Fig. 2. First, the ADC was measured along both directions while the long axis of the tendon was perpendicular to B_0. Then the tube holding the tendon was rotated, so that the long axis of the tendon was oriented parallel to B_0. The ADC was again measured along both directions. The resulting values of ADC along the long and short axes of the tendons are shown in Fig. 7. Changing orientation had little effect on the ADC along the perpendicular direction of the tendon (3.5 versus 3.1×10^{-6} cm^2/s). However, the ADC values along the parallel direction of the tendons were significantly different (7.3 ± 0.4 versus $5.6 \pm 0.6 \times 10^{-6}$ cm^2/s, $P = 0.024$).

2. Mechanical Testing

The mechanical testing experiments were done in order to describe the mechanical behavior of tendons under conditions similar to those used in the NMR experiments.

a. Length–force tests. We wanted to determine whether the loads we used in the NMR experiments caused stresses in the physiological range. The relationship between length and force was measured in four PBS-stored tendons. Data from one representative tendon are shown in Fig. 8. Application of a 10-N load caused stresses in the range of 1.5 MPa. The nonlinear shape of the stress–strain curve indicates that stresses used in these experiments are at the lower (physiological) end of the stress–strain function (*14*).

b. Creep tests. We wanted to determine whether the time constants of creep and recovery were similar to the time

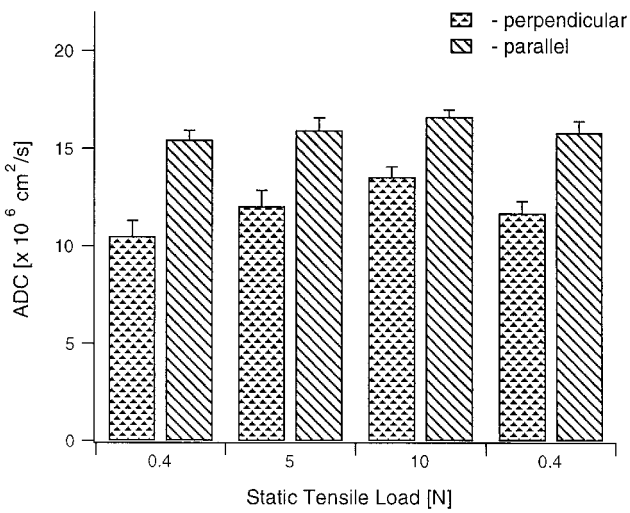

FIG. 4. $ADC_\perp$ and $ADC_\parallel$ values in PBS-stored rabbit Achilles tendons under static tensile loads. The diffusion time for these data was $t = 80$ ms. Loads were presented in the sequence denoted along the horizontal axis. The error bars are ±SEM, $N = 30$.

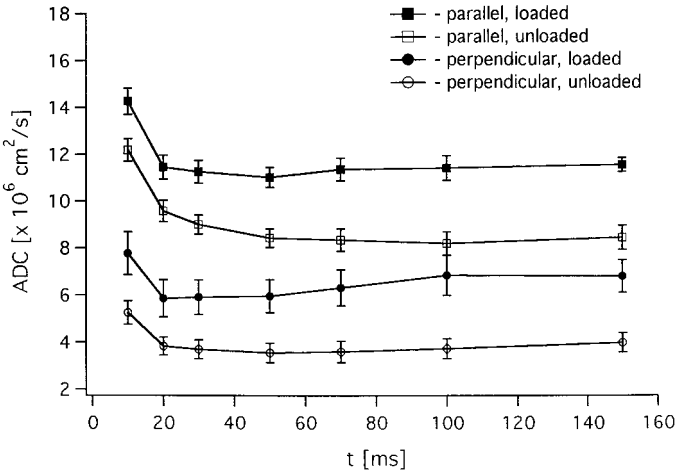

FIG. 5. Effect of diffusion time and loading upon ADC of tendon water in fresh rabbit Achilles tendons. Diffusion was measured both parallel and perpendicular to the major axis of the tendon. Data denoted as "loaded" had an applied load of 5 N. Error bars are ± SEM, $N = 10$.

constants of the changes that we observed in ADC in the NMR experiments. Creep tests were done on five fresh tendons. Data from a single representative tendon are shown in Fig. 9. Upon application of a tensile load, the tissue elongated. The longest time constants of the elongation ($N = 5$) and recovery ($N = 4$) processes had values between 4 and 6 min. The mean time constants for elongation and recovery were not significantly different. Recovery was never complete within the time course of the experiments; each tendon showed evidence of residual strain at the end of the recovery period. The residual strain had a mean magnitude ($N = 4$) of 0.17.

Creep tests on PBS-stored tendons were conducted with the tissue under paraffin oil, so that conditions would be similar to those of the NMR experiments. The tendons were observed visually during these tests. During one test, extruded fluid accumulated in the form of a drop such that it was observable (Fig. 10).

3. Electron Microscopic Measures of Fibril Size and Spacing

Analysis of fibril size and spacing was done using one image from each of the four tendons fixed while unloaded and the four fixed under load. Examples of sections taken from loaded and unloaded tendons are shown in Fig. 11. The number of fibrils and the diameters of fibrils were determined in defined areas of the images. The mean fibril size was determined from measures of approximately 1000 fibrils; mean fibril diameter ($N = 988$) was 0.14 ± 0.0038 μm in unloaded and 0.13 ± 0.0003 μm ($N = 1114$) in loaded tendons. Although small, the difference was highly significant ($t = 3.64$; df = 2100; $P = 0.0003$). The space between fibers was 0.37 of the total area in control tendons and 0.40 in tensile-loaded tendons.

DISCUSSION

The changes in ADC that we observed are interpreted in terms of a water-transport phenomenon. In our model, tensile loading causes extrusion of water from the inside of the tendon to a bulk phase along the outside surface of the tendon. The water in the bulk phase has a high ADC and is consistent with the increase in ADC that we observed with loading. Our interpretation is consistent with a general model of the behavior of fluids in soft tissues under load, since it has been shown that fluid is extruded from cartilage when it is loaded in compression (*1*). Here we show evidence for similar (i.e., load–evoked) water transport, in the more general case of a soft tissue structure loaded in tension.

Our findings are all based on spectroscopic measurements made from whole tendons, i.e., including the tendon, its sheath, and the space along the outside surface. Because of the low water content and short T_2 of tendon (*15*) we chose to collect signals from the entire tendon. It should be recognized, however, that there are a number of limitations associated with this method. For example, while we believe that water movement is the main effect of loading, it is not directly measured with this method. Experiments done using imaging or experiments in which the extruded fluid is removed (*16*) would allow a more direct measure of a transport phenomenon. Also, since whole tissue spectroscopy aggregates measures from all compartments of the structure, most notably the tendon and any ex-

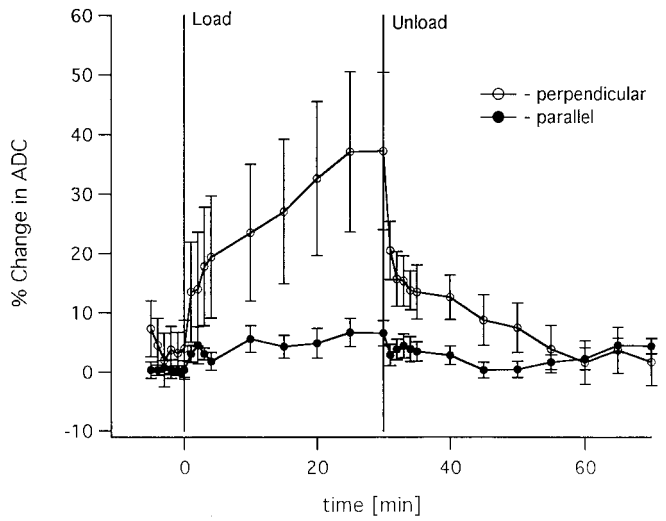

FIG. 6. Transient response of ADC caused by tensile loading of fresh rabbit Achilles tendons ($N = 10$, error bars are ±SEM). Data for each tendon were expressed as a percentage of control; the graph shows the mean of those percentages across 10 tendons. The points marked "load" and "unload" represent the application and removal points of a 5-N tensile load. The significance of changes in the ADC was evaluated using repeated-measures ANOVA by comparing the five values recorded prior to load application to the three values recorded between 20 and 30 min following load application, when the ADC change had reached a relatively steady state. The increases along both directions were highly significant ($P < 0.001$).

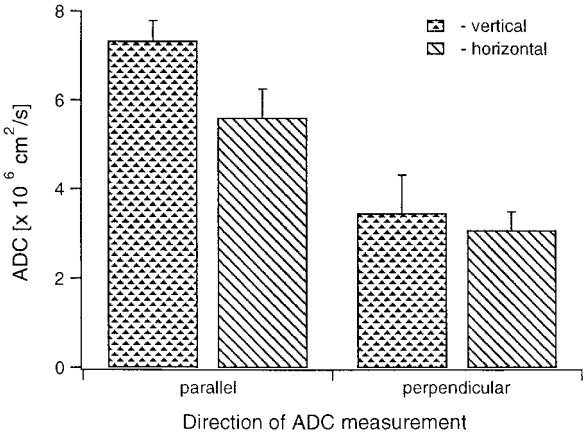

FIG. 7. Dependence of the ADC of rabbit Achilles tendon water ($N = 4$) on tendon orientation in the magnet. Data were acquired with the apparatus shown in Fig. 2. The diffusion time was 80 ms. Tendon long axis and tendon short axis refer to the ADC measured along the parallel axis and the perpendicular axis of the tendon, respectively. The error bars are ±SEM. $ADC_{\parallel}$ values were statistically different ($P = 0.024$) while the $ADC_{\perp}$ values were not.

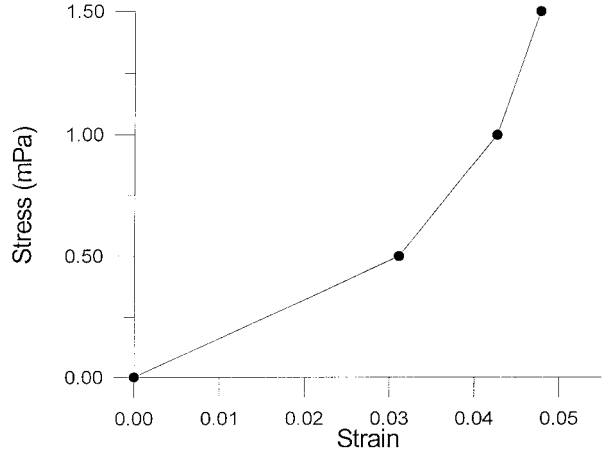

FIG. 8. Stress–strain curve for a PBS-stored rabbit Achilles tendon, using loads up to 10 N. Application of a 10-N load caused stresses in the range of 1.5 MPa. The nonlinear shape of the stress–strain curve indicates that stresses used in the NMR experiments are at the low (physiological) end of the stress–strain function.

truded fluid, it is impossible to quantify the magnitude of fluid extrusion. An additional limitation is that the method is only applicable in experiments in which extruded water can accumulate stably along the outside of the tendon. It would not be suitable (for example) in an *in vivo* experiment where extruded fluid might be transported away from the tendon sheath. Despite these shortcomings, the spectroscopic measure allows for fast measurements, allowing us to follow the response in the loading-time domain with 60 s resolution.

The finding of anisotropic diffusion of water in rabbit Achilles tendon in the present experiment conflicts with the finding of diffusional isotropy by Henkelman *et al.* (*17*) in experiments on bovine Achilles tendon. In comparison, we found strong anisotropy. At a diffusion time of 19.0 ms, Henkelman *et al.* found an ADC value of $13.7 \pm 1.5 \times 10^{-6}$ cm^2/s along both perpendicular and parallel directions. This value is larger than our measurement of the parallel direction ADC in fresh tendon $9.6 \pm 0.4 \times 10^{-6}$ cm^2/s (mean ± SEM, $N = 9$).

One possible explanation for the difference between the above results is that in the experiments of Henkelman *et al.* the sample, not the gradient direction, was rotated to measure the ADC in perpendicular directions. The strong orientation of the sample fibrils may cause an angular dependence of magnetic susceptibility patterns, resulting in a similar ADC value in each perpendicular direction. In Henkelman's work, the T_2 relaxation time was found to vary as the angle between the long axis of the tendon and the direction of B_0 was changed from 0 to 55 to 90° in agreement with the trend and values observed by Fullerton *et al.* (*18*). Since T_2 is known to be sensitive to susceptibility gradients in tissue, this could affect the diffusion measurements since spin populations with short T_2's would be removed for the value of TE used in these experiments. It is possible that different populations of spins would be removed at different orientations. In addition, the tendons used by Henkelman *et al.* were not surrounded by fluid. The resulting glass–air sample interfaces would result in a larger susceptibility difference than in our experiment.

In the experiments in which we rotated both the specimen and the fields, we found that there was no statistically significant difference in $ADC_{\perp}$ between the two orientations (Fig. 4). However, the ADC values along the parallel direction of the tendons differed significantly ($P = 0.024$) between the two orientations. While it is unclear why different results were obtained for the parallel and perpendicular directions with respect to B_0, these results demonstrate that a consistent orientation of the tendon in the magnet is important when comparing ADC values for different directions. Since the gradient, not the sample direction, was varied in the present experiments, changing magnetic susceptibility patterns should not affect our results.

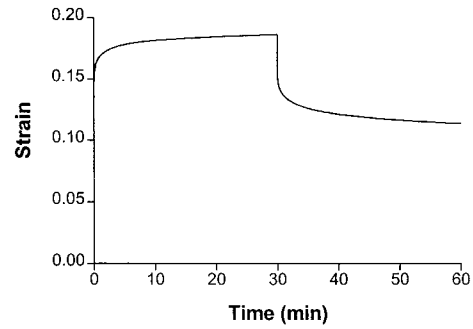

FIG. 9. Tendon elongation and recovery observed during a creep test on a fresh rabbit Achilles tendon bathed in paraffin oil. The applied load was 5 N (the stress was 0.8 MPa). At the end of the recovery phase of the test there was a residual strain of 0.12.

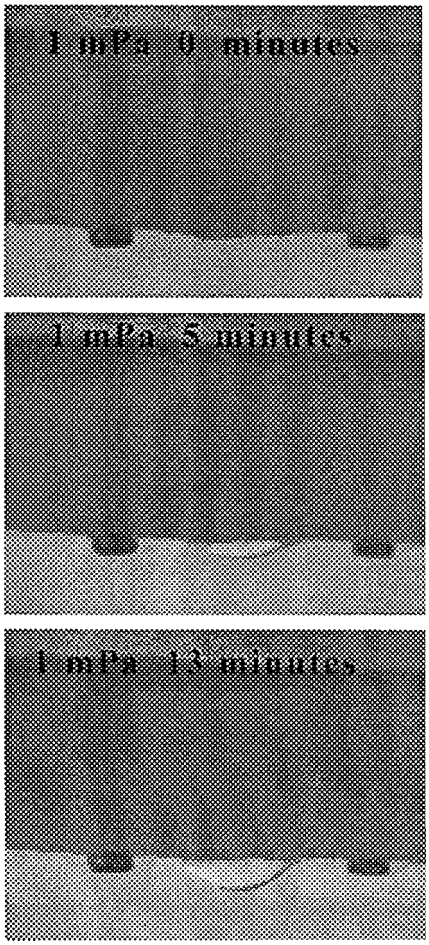

FIG. 10. Photographs showing the extrusion of bulk water from a PBS-stored rabbit Achilles tendon under a 1-MPa tensile stress (load = 6.2 N). Top: 0 min. Middle: 5 min after application of load. Bottom: 13 min after application of load.

The anisotropy differences between the parallel and perpendicular directions can be accounted for in terms of the tendon's structural anisotropy. The collagen component of the solid matrix offers fewer barriers to diffusion along the parallel direction, while the diffusion path along the direction orthogonal to the fiber orientation is significantly more restricted (see Fig. 11).

The measured ADC values in Table 3 were greater in PBS-soaked tendons than in fresh tendons. This reflects swelling of the PBS-stored tendons, since 300 mOsM PBS is hypo-osmotic and results in greater tendon water content. This osmotic swelling would presumably increase the distance between barriers to diffusion and, therefore, increase the ADC. The effect of this can be seen by comparing Figs. 4 and 5. The ADC values in each direction are higher for the PBS-soaked tendons and the effect of loading is relatively smaller on their already-elevated ADC values. Freezing (which was used with the PBS-stored tendons) might also increase the ADC since ice crystal formation may disrupt cell membranes (and perhaps also the tendon structure) and thus reduce the barriers to diffusion. The results of the present experiments suggest that if water content is an important factor in determining a tissue's material properties, the use of freshly isolated, paraffin-oil-stored material is preferable to the PBS-stored samples that are commonly used in the study of gross tissue mechanics (*19*). The large variation in values of ADC between tendons that is seen in Table 3 is of unknown origin. Potential contributors would be the use of different tendons from different animals and differing amounts of water lost during preparation and mounting in the apparatus.

The ADC increased with applied load. On the one hand, this could be the result of decreasing the packing of the structural components of the tendons. Electron microscopic observations showed that area between fibrils was slightly greater (37% vs

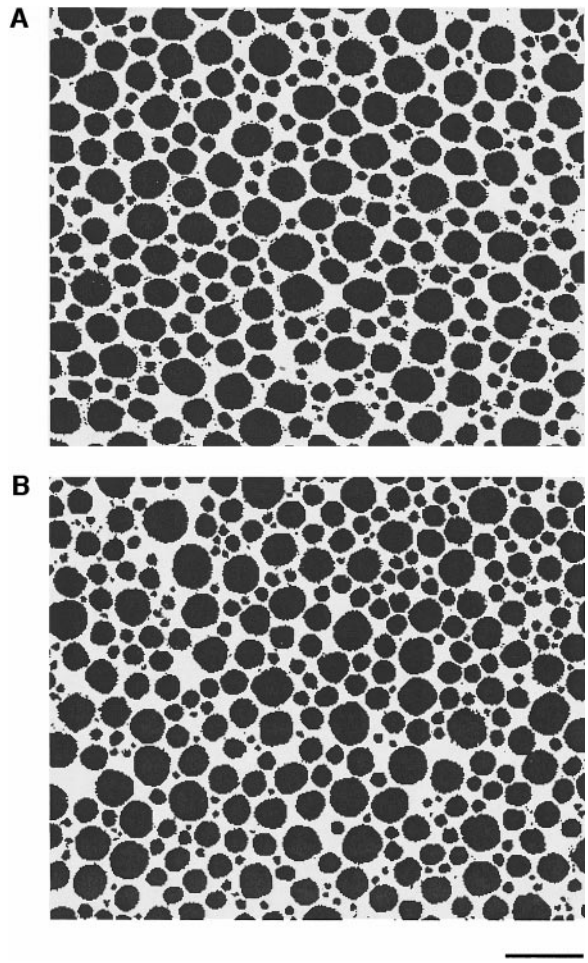

FIG. 11. Representative transmission electron micrographs of unloaded (A) and loaded (B) rabbit Achilles tendons. Applied load was 10 N. The contrast of the micrographs has been changed so that fibrils are black while the background is white. Length marker: 0.5 μm. Mean fibril diameter was 0.14 μm ($N = 988$) in the micrograph of the unloaded tendon and 0.13 μm ($N = 1113$) in the micrograph of the loaded tendon. The difference was highly significant ($P < 0.001$). The space between fibers was 0.37 of the total area in control tendons and 0.40 in loaded tendons.

40% of the total area) in tendons fixed under a 10.4-N load. We have estimated the increase in ADC measured in the perpendicular direction that would be caused by this decrease in packing. We assumed that the space available for diffusion between fibrils is roughly cylindrical. Using the expression derived in Söderman and Jönsson (*20*) for signal attenuation for the case of diffusion perpendicular to the long axis of the tendon, we find roughly a 9% increase in the perpendicular ADC in response to the observed increase in area between the fibrils. Even though electron micrographs sample a very small region of tendon, making it possible that the results may not be representative of the packing in all regions of the tendon, this increase appears to be too small to account for the observed changes in the ADC with loading. Because of this, we favor the interpretation that loading causes water extrusion from the tendon, with the accumulation of water in a bulk phase along the outside surface of the tendon. Since the NMR measurement aggregates both the bulk and the tendon water phases, the result of an extrusion process would be an increase in the ADC. This extruded water is included in the ADC measurements since this water is confined to the tendon surface by the paraffin-oil bath. This interpretation is supported by the observation, in one experiment, of bulk extruded fluid outside the tendon. Also in support of this interpretation is the fact that the ADC increased with load over the range of measured diffusion times.

As bulk water, the extruded fluid would have a diffusion coefficient of $\sim 1.9 \times 10^{-5}$ cm^2/s (based upon the temperature at which the experiment was performed), much greater than the ADC of the water interior to the tendon. Burstein *et al.* (*16*) showed a decrease in water ADC value when cartilage was loaded in compression. However, our results are not necessarily in conflict with their findings since they removed the extruded fluid before measuring the ADC. In the present set of experiments, the spatial distribution of ADC values was not measured and, therefore, if a similar drop in ADC does occur in tendon, it is somewhat masked by the signal from the extruded water.

The stress–strain curve for tendon has a nonlinear toe region at low stresses, a linear region at intermediate stresses, and a failure region at high stresses (*14*). The ultimate strength of Achilles tendons in rabbits of this age is 20–60 MPa (*21, 22*). Thus, the stresses that we used (up to 1.5 mPa) were in the toe region and possibly extended into the beginning of the intermediate region. The stresses were at least an order of magnitude below the ultimate stress for these tendons. Thus we conclude that the changes in ADC were not a result of injury to the tendon.

It has been shown that structural information may be obtained from the behavior of the ADC as t is varied (*9, 10*). This fact may be understood by noting that the reduction of the diffusion coefficient from D_0, the bulk fluid value, to ADC ($<D_0$) is due to reduction in the mean-squared displacement of the water molecules as they encounter obstacles to their motion. As the diffusion time is increased, the fraction of molecules that encounter diffusion obstacles also increases. Therefore, the rate at which the ADC changes with respect to t should reflect, albeit indirectly, the structural organization of the sample. At long diffusion times, this curve reaches a constant value, D_{eff}, as the water molecules have all experienced the same degree of restriction. The value at which the curve levels out reflects the tortuosity of the sample, $D_{\text{eff}} = D_0/T$, where D_0 is the value of the bulk fluid diffusion coefficient and T is the tortuosity. The tortuosity is a measure of the connectivity of the space available for diffusion in a given direction. In tendon, T reflects both the cell membrane permeability (in tendons, mostly fibrocytes) and the diffusion in the extracellular matrix.

Note in Fig. 5 that both $\text{ADC}_\perp$ and $\text{ADC}_\parallel$ for unloaded tendons become constant at longer times, while the data for the loaded tendons do not. The increase in ADC at larger t values is consistent with the existence of extruded fluid. It should be noted, however, that the extruded water signal does not overwhelm the signal from the water still interior to the tendon. The effect of the extruded water seems to be that of a constant offset in the ADC value. This is not surprising, since the extruded water signal is not likely to show any diffusion-time dependence if it is in a bulk phase. It should be noted that, because of this lack of diffusion-time dependence for the extruded water, the shape of the ADC versus t curve is still fully reflective of the water interior to the tendon, at least at the shorter values of t. In addition, the magnitudes of the ADC versus t curves for the parallel and perpendicular directions are, due to the water extrusion, only comparable within the same state, i.e., that magnitudes of $\text{ADC}_\perp$ and $\text{ADC}_\parallel$ are only comparable for either the loaded or the unloaded conditions, but not between different loading conditions.

Because the extruded water is expected to add only a constant value to the total water ADC, calculation of anisotropy ratios from tendon in the loaded state is not indicative of only the water interior to the tendon, since, as an additive constant the ADC of the extruded water does not divide out when the ratio $(\text{ADC}_\parallel(\text{interior}) + \text{ADC}_\parallel(\text{extruded}))/(\text{ADC}_\perp(\text{interior}) + \text{ADC}_\perp(\text{extruded}))$ is formed. It was found, however, that the calculated anisotropy ratio decreases only slightly upon loading. The difference $\text{ADC}_\parallel - \text{ADC}_\perp$ for all values of t yields a value independent of the amount of extruded water since the values in both curves should be elevated by the same amount after extrusion.

The rise in the ADC of the loaded samples at larger t values is most likely due to the elimination of one population of water molecules with relatively short T_1 values. As the diffusion time is increased, the TM period in the stimulated-echo sequence is increased and T_1 decay will occur. The signal arising from water molecules with relatively shorter T_1 values will be preferentially attenuated as the diffusion time is increased. The amount of attenuation due to T_1 decay is the same in either direction, but differs between unloaded and loaded data. The

attenuation in M_0 value between $t = 21.0$ ms and $t = 400$ ms was ~84% for the unloaded cases and ~68% for the loaded case. This shows that at longer diffusion times the signal is heavily weighted toward the water molecules with the longest T_1 values and that there are more molecules with longer T_1 values in the loaded case.

Looking at the data for the unloaded tendons, it can be seen that $ADC_\perp$ becomes constant at a shorter diffusion time than does $ADC_\parallel$. This implies that the characteristic length scale of the restrictions is smaller in the perpendicular direction than in the parallel direction. This is consistent with the oriented structure of the tendon and the reduced $ADC_\perp$ versus $ADC_\parallel$ for all diffusion times measured here. It is important to note that structural information is still present even with the contribution to the measured ADC by the extruded water. It is most apparent at diffusion times in the middle of our range, however, before the signal becomes heavily T_1 dependent.

If the value of D_0 (the bulk value of tendon water) were known, the characteristic length scale in each direction could be estimated through the Einstein relation ($\langle (r - r')^2 \rangle = 2Dt$, where $\langle (r - r')^2 \rangle$ is the mean-squared displacement of an ensemble of molecules in one dimension, D is the self-diffusion coefficient, and t is the diffusion time) by equating the square root of the mean-squared displacement with the characteristic length in a given direction and using D_0 for the diffusion coefficient. However, even though D_0 is not known, an estimate of the ratio of characteristic length scales can be found using the ratio of the square roots of the mean-squared displacements: $(\langle (r - r')^2 \rangle_\parallel / \langle (r - r')^2 \rangle_\perp)^{1/2} = (t_\parallel / t_\perp)^{1/2} \cong (0.05 \text{ s}/0.02 \text{ s})^{1/2} = 1.6$. Here we have used the diffusion times at which the ADC vs t curve becomes constant.

The increase in both $ADC_\perp$ and $ADC_\parallel$ for the longest diffusion times after loading is also consistent with the idea of water transported to a bulk phase. During the period between the second and third 90° pulses in the PFG STE sequence, T_1 decay will occur. This decay will weight the observed signal to the distribution of water molecules having the longest T_1 values and, presumably, the fewest restrictions to diffusion. This would tend to increase the ADC with increasing diffusion time. This effect would be accentuated in the case of extruded water since the extruded fluid would have a T_1 value longer than that of the fluid still residing in the tendon. As t increases the weighting of the signals arising from the tendon water and the extruded water would shift to an increased extruded water contribution.

Following the application of a load, the ADC increased along both parallel and perpendicular directions. However, the increase was greater in the perpendicular direction (~37%) than in the parallel direction (~7%) (Fig. 6). We attribute this to the geometry of the tendon. The greater increase in $ADC_\perp$ is consistent with the idea that, since the water molecules are more restricted in the perpendicular direction, the addition of bulk fluid to this ensemble of water molecules results in a proportionally greater change in the measured ADC.

In transient tests, the ADC changed and the tendons displayed creep (elongation) responses. The ADC changed with time constants of 13 and 17 min for loading and unloading, respectively. The rate of ADC increase was greatest in the 5 min after loading and then decreased until the load was removed at 30 min. Since it is likely that water transport and extruded water are causing the increase in ADC, it is clear that these processes begin within 1 min after loading. We undertook transient, mechanical creep tests in order to determine whether the ADC might be directly related to an elongation response. However in similar transient tests, tissue elongation and recovery had quite different time constants, on the order of 4 to 6 min. Furthermore, upon unloading the ADC returned to baseline values while the mechanical response did not. These results imply that water extrusion is not simply coupled to mechanical deformation of the tendon.

Since we have shown that tendons elongate under the conditions of this experiment, it is a concern that sample motion might influence the results. The effect of material stretching on a diffusion measurement is to reduce the diffusion encoding, resulting in a reduction in the observed ADC (*23*). The magnitude of any such effect is related to the magnitude of the motion in relation to the time period over which the ADC measurement is made. Several factors argue against a role for motion artifacts in these results. First, material elongation was slow, having time constants on the order of minutes. In contrast, the diffusion times were on the order of milliseconds to hundreds of milliseconds. Further, in order to minimize the effects of sample motion on these results, the static tests used a delay of 15 min between the application of the load and the measurement of the ADC. Thus, it is unlikely that significant, nondiffusional motion occurred in the measurement period of these experiments.

ACKNOWLEDGMENTS

This work was supported by USPHS Grant NS-10783. Special thanks are extended to Arthur Allard, who built the apparatus.

REFERENCES

1. V. C. Mow, M. H. Holmes, and W. M. Lai, Fluid transport and mechanical properties of articular cartilage: A review. *J. Biomech.* **17,** 377–394 (1984).
2. A. Viidik and T. Lewin, Changes in tensile strength and histology of rabbit ligaments induced by different modes of postmortal storage. *Acta Orthop. Scand.* **37,** 141–155 (1966).
3. J. Galante, Tensile properties of the human annulus fibrosis. *Acta Orthop. Scand. Suppl.* **100,** 1–91 (1967).
4. D. F. Betsch and E. Baer, Structure and mechanical properties of rat tail tendon. *Biorheology* **17,** 83–94 (1980).
5. H. R. Elden, Hydration of connective tissue and tendon elasticity. *Biochim. Biophys. Acta* **79,** 592–599 (1964).
6. D. Chimich, N. Shrive, C. Frank, L. Marchuk, and R. Bray, Water content alters viscoelastic behaviour of the normal adolescent rabbit medial collateral ligament. *J. Biomech.* **25,** 831–837 (1992).

7. J. A. Hannafin and S. P. Arnoczky, Effect of cyclic and static tensile loading on water content and solute diffusion in canine flexor tendons: an in vitro study. *J. Orthop. Res.* **12,** 350–356 (1994).
8. M. D. Hurlimann, K. G. Helmer, T. M. de Swiet, P. N. Sen, and C. H. Sotak, Spin echoes in a constant gradient and in the presence of simple restriction. *J. Magn. Reson.* **113,** 260–264 (1995).
9. P. P. Mitra, P. N. Sen, and L. M. Schwartz, Short-time behavior of the diffusion coefficient as a geometrical probe of porous media. *Phys. Rev. B* **47,** 8565–8574 (1993).
10. D. L. Johnson, T. J. Plona, C. Scala, F. Pasierb, and H. Kojima, Tortuosity and acoustic slow waves. *Phys. Rev. Lett.* **49,** 1840–1844 (1982).
11. P. J. Hore, Solvent suppression in Fourier transform nuclear magnetic resonance. *J. Mag. Reson.* **32,** 283–300 (1983).
12. J. J. Duquette, P. Grigg, and A. H. Hoffman, The effect of diabetes on the viscoelastic properties of rat knee ligaments. *J. Biomech. Eng.* **118,** 557–564 (1996).
13. Y. C. Fung, *in* "Biomechanics—Mechanical Properties of Living Tissues," pp. 242–310, Springer-Verlag, New York (1993).
14. A. Viidik, Properties of tendons and ligaments, *in* "Handbook of Bioengineering," (R. Skalak and S. Chien, Eds.), pp. 6.1–6.19, McGraw–Hill, New York (1987).
15. T. M. Haygood, Magnetic resonance imaging of the musculosketal system: 7. The ankle. *Clin. Orthop.* **336,** 318–336 (1997).
16. D. Burstein, M. L. Gray, A. L. Hartman, R. Gipe, and B. D. Foy, Diffusion of small solutes in cartilage as measured by nuclear magnetic resonance (NMR) spectroscopy and imaging. *J. Orthop. Res.* **11,** 465–478 (1993).
17. R. M. Henkelman, G. J. Stanisz, J. K. Kim, and M. J. Bronskill, Anisotropy of NMR properties of tissues. *Magn. Reson. Med.* **32,** 592–601 (1994).
18. G. D. Fullerton, I. L. Cameron, and V. A. Ord, Orientation of tendons in the magnetic field and its effect on T2 relaxation times. *Radiology* **155,** 433–435 (1985).
19. T. Yamaji, R. E. Levine, S. L. Woo, C. Niyibizi, K. W. Kavalkovich, and C. M. Weaver-Green, Medial collateral ligament healing one year after a concurrent medial collateral ligament and anterior cruciate ligament injury: an interdisciplinary study in rabbits. *J. Orthop. Res.* **14,** 223–227 (1996).
20. O. Söderman and B. Jönsson, Restricted diffusion in cylindrical geometry. *J. Magn. Reson. A* **117,** 94–97 (1995).
21. T. A. L. Wren, G. S. Beaupre, and D. R. Carter, A model for loading-dependent growth, development, and adaptation of tendons and ligaments. *J. Biomech.* **31,** 107–114 (1998).
22. Y. Nakagawa, K. Hayashi, N. Yamamoto, and K. Nagashima, Age-related changes in biomechanical properties of the Achilles tendon in rabbits. *Eur. J. Appl. Physiol.* **73,** 7–10 (1996).
23. T. G. Reese, V. J. Wedeen, and R. M. Weisskoff, Measuring diffusion in the presence of material strain. *J. Magn. Reson. B.* **112,** 253–258 (1996).